

Design and Implementation of Photovoltaic Electric Vehicle Charging Stations: A Case Study at Universidad Tecnológica de Pereira

Edgar Salazar¹ and Oscar Gómez¹

¹ Facultad de Tecnología
Universidad Tecnológica de Pereira
Pereira, Colombia

Abstract. As the global transportation sector transitions towards sustainability, the need for renewable energy-powered electric vehicle (EV) charging infrastructure becomes increasingly evident. This paper presents a case study on the design and implementation of a photovoltaic electric vehicle charging stations at the Universidad Tecnológica de Pereira (Colombia). The study outlines the design process, technical specifications, and implementation strategies for a photovoltaic (PV) charging station, emphasizing key considerations such as location selection, solar panel configuration, and necessary equipment. Additionally, the paper evaluates the performance and effectiveness of the PV charging station in supplying the demand for EV charging services on campus. This case study provides valuable insights into the feasibility and scalability of PV EV charging infrastructure in educational institutions.

Key words. Photovoltaic, charging station, electric vehicle.

1. Introduction

In recent years, the global transportation sector has witnessed a paradigm shift towards sustainable alternatives, primarily motivated by concerns over environmental degradation and the imperative to mitigate climate change. One of the most promising solutions to emerge from this transition is the widespread adoption of electric vehicles (EVs). Unlike traditional internal combustion engine vehicles, EVs offer a cleaner, more efficient mode of transportation, significantly reducing harmful emissions, lessening reliance on finite fossil fuels and substantial reduction in greenhouse gas emissions and air pollutants associated with traditional gasoline-powered vehicles.

However, the widespread adoption of EVs also presents a set of challenges, chief among them being the development of adequate charging infrastructure. As the number of EVs grows, so does the demand for charging stations. Without a comprehensive network of charging infrastructure, EV adoption could be hindered, potentially impeding the transition to a sustainable transportation system.

The environmental impact of conventional charging stations powered by the grid cannot be overlooked. While EVs themselves produce zero emissions during operation, the electricity used to charge them often comes from fossil fuel sources, negating some of the environmental benefits of EVs. To address this issue, there is a growing need to explore alternative charging solutions that leverage renewable energy sources such as solar power.

Recent studies have focused on the design and implementation of chargers of battery EV using solar energy. For example, [1] investigates the possibility of charging battery electric vehicles at workplace in Netherlands using solar energy; [2] plug and play solar photovoltaic (PV) power plant to charge electric vehicles (EVs) is proposed and modelled using MATLAB/Simulink software; [3] investigates the solar potential, charging tariff, and associated costs of solar charging stations in Bangladesh; [4] introduces a new simple analysis and design of a standalone charging station powered by PV energy; and [5] investigates the economic viability of grid-connected PV systems for EV charging stations in Ngawi City, Indonesia.

This paper discusses the key factors to consider when designing PV EV charging stations, details the required components, and explain the architecture of the system and how these components interact; also, provides a detailed technical description of the design and implementation process, and presents the results of performance evaluations, including efficiency, charging capacity, and economic and environmental impact.

2. Photovoltaic EV Charging Station Design

A charging station will be designed for Mode 3 charging technology with a Wallbox of 3.7 kW expandable to 11.4 kW. The connector will be Type 2 (or Mennekes), which allows charging for a wide variety of European vehicles. In addition, a single-phase output for Type 1 connector with Mode 1 charging technology will be provided to charge converted electric vehicles (vehicles that were originally combustion-based).

To determine the required solar system for a full daily charge, the availability of irradiation at the planned installation location is assessed. Based on irradiance sensor data (W/m^2), measurements are taken every 5 minutes over 3 years. Figure 1 shows a curve obtained with irradiation data.



Fig. 1. Irradiation (W/m^2) in the installation place.

The annual average daily irradiation is calculated to estimate the available solar peak hours (SPH) at the site. This value is obtained by calculating the area under the irradiance vs. time curve (Figure 1). A trapezoidal sum point-to-point of all the data obtained each day is done to get an annual average daily of $4,3 \text{ kWh}/m^2$.

$$\text{Available energy} = W_{\text{panel}} \times \text{SPH} \times \text{efficiency} = 12 \text{ kWh} \quad (1)$$

Thus, W_{panel} is equal to 3.5 kWp , considering a 20% loss in capture due to the panel location ($4^\circ 47' 35,2'' \text{ N}$ $75^\circ 41' 22,8'' \text{ W}$). A 3.6 kW PV system consisting of nine panels of 400 Wp (Watts peak).

The nine panels occupy an area of 18.13 m^2 . The available roof space at the planned location is 21 m^2 ; therefore, it is suitable for installation in a 3×3 panel array. An on-grid system is projected to allow the grid to power the charging station when PV generation is insufficient to power the EV charging. Additionally, any unused PV energy for EV charging station will be sent to the distribution system, and through a bidirectional meter, the energy balance will be stored and monitored over time.

The location, orientation, and tilt of the panels will be towards the south. An inclination of 8° is projected to achieve a balance between the local average latitude ($4^\circ 47' \text{ N}$) and the required tilt to efficiently drain rainwater and moisture. Figure 2 presents the panel performance parameters.

MECHANICAL SPECIFICATION		ELECTRICAL CHARACTERISTICS	
Format	2015mm x 1000mm x 35mm (including frame)	Power at MPP ¹	P_{MPP} [W] 400
Weight	23.5kg	Short Circuit Current ¹	I_{sc} [A] 10.19
Front Cover	3.2mm thermally pre-stressed glass with anti-reflection technology	Open Circuit Voltage ¹	V_{oc} [V] 48.96
Back Cover	Composite film	Current at MPP	I_{MPP} [A] 9.70
Frame	Anodised aluminium	Voltage at MPP	V_{MPP} [V] 41.23
Cell	6 x 24 monocrystalline Q.ANTUM solar half cells	Efficiency ¹	η [%] ≥ 19.9
Junction box	53-101mm x 32-60mm x 15-18mm Protection class IP67, with bypass diodes		
Cable	4mm ² Solar cable, (+) $\geq 1350\text{mm}$, (-) $\geq 1350\text{mm}$		
Connector	Stäubli MC4-Evo2-IP68		
TEMPERATURE COEFFICIENTS			
Temperature Coefficient of I_{sc}	α [%/K] +0.04	Temperature Coefficient of V_{oc}	β [%/K] -0.27
Temperature Coefficient of P_{MPP}	γ [%/K] -0.35	Normal Module Operating Temperature	NMOT [°C] 43 ± 3

Fig. 2. Technical data of the projected panels.

To receive the electrical photovoltaic generation in DC and convert it into AC, a $3,8 \text{ kW}$ on-grid inverter is considered. Also, it is required a vehicle charger, a

bidirectional meter, and an electrical connection board with terminals for three-phase AC connection for the energy entering the inverter through the panels, and the energy exiting to the distribution system through the bidirectional meter (the energy direction can also be from the distribution system to the load). Figure 3 presents the specifications of the projected inverter.

INPUT DATA		PRIMO 3.8-1	
Recommended PV power (kWp)		3.0 - 6.0 kW	
Max. Usable input current (MPPT 1 / MPPT 2)		18 A / 18 A	
Total max. DC current			
Max. array short circuit current (1.25 Imax) (MPPT 1 / MPPT 2)			
Operating voltage range			
Max. input voltage		410	
Admissible conductor size DC			
MPP Voltage Range		200 - 480 V	
OUTPUT DATA		PRIMO 3.8-1	
Max. output power	240 V	3800 W	
	208 V	3800 W	
Max. continuous output current	240 V	15.8 A	
	208 V	18.3 A	
Recommended OCPD / AC breaker size	240 V	20 A	
	208 V	25 A	
Max. Efficiency		96.70%	
CEC Efficiency	240	95.00%	

Fig. 3. Technical data of the projected inverter.

The connection of panels in series will ensure the required DC input voltage, as shown in (2):

$$\begin{aligned} \text{Voltage } MPP \times 9 &= 41,23 \text{ V} \times 9 = 369,4 \text{ V} \\ \text{Voltage } Voc \times 9 &= 48,96 \text{ V} \times 9 = 440,6 \text{ V} \end{aligned} \quad (2)$$

Considering the variation of voltage with temperature coefficient (Fig 2): $V_{ocmin} = 440,6 \text{ V} (1 - 0,27\%/K \times 23K) = 413,2 \text{ V}$. $V_{ocmax} = 440,6 \text{ V} (1 - 0,27\%/K \times 3K) = 437 \text{ V}$. This value is between the required range for the inverter ($200 \text{ V} - 480 \text{ V}$), even considering the panel temperature variation, which has seen measured between 10°C and 40°C . With these temperature variations, both the power and voltage remain within the required range.

Additionally, the series arrangement allows the maximum current generated in the solar panels to be equivalent to the value generated by one panel. According to the panel catalogue, $I_{max} = I_{sc}$ (short circuit) = $10,24 \text{ A}$, which is lower than the maximum DC current accepted by the inverter (18 and 36 A in each MPPT input). Figure 4 shows the single-line diagram of the proposed design.

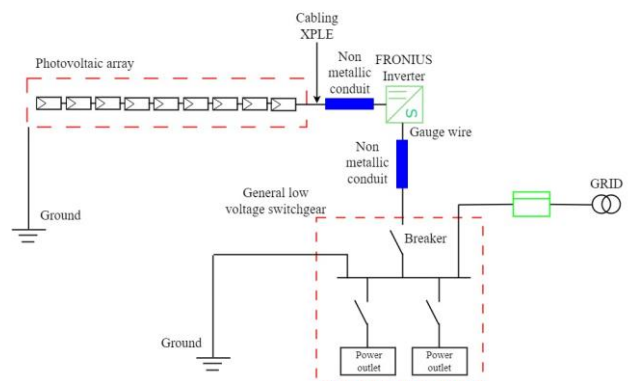


Fig. 4. Single-line diagram for the $3,6 \text{ kW}$ Solar-Powered Electric Vehicle Charging Station.

3. Photovoltaic EV Charging Station Implementation

After selecting the site, the resistance of the structure supporting the roof is verified. The weight of each panel is 24 kg, so the structure must support a weight of 216 kg over a length of 6 meters, resulting in a distributed load of 352 N/m, which, in addition to the roof, does not exceed the maximum permissible values for the 3 beams that support the structure. The roof inclination is approximately pointing towards the north; therefore, the installation of additional structure was required to raise the panels, achieving a southward inclination to maximize the average daily annual radiation. Figure 5 shows the final assembly.



Fig. 5. Final Presentation of PV electric charging station

Figure 6 depicts the weather station equipped with sensors for monitoring solar radiation, wind speed, environment temperature, and panel temperature (thermocouple attached to the underside of the panel). This unit was strategically positioned on the upper front part of the station to guarantee unobstructed visibility and proximity to the power source (120 V AC).

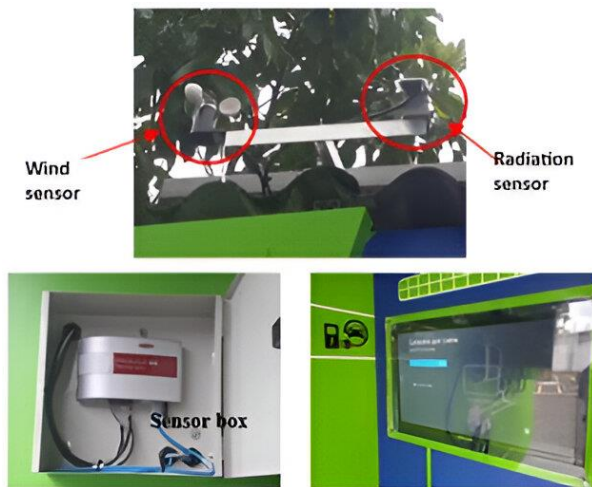


Fig. 6. Atmospheric variables measurement unit and display.

Additionally, a display is included, which presents real-time curves of the energy and meteorological variables of the system. Finally, the sensor box is an electronic device

to energize and manages signals obtained from the weather station.

The effect of environment temperature and the influence of wind speed on the panel temperature and consequently on its generation capacity can be analyzed. In general, PV panels increase their voltage with increasing temperature and vice versa. The increase in panel temperature raises the short-circuit current (I_{sc}), decreases the power at the maximum power point (MPP), and reduces the open-circuit voltage (V_{oc}). The opposite effect occurs with a decrease in temperature. However, within the environment temperature range of the site, voltage, current, and power values will remain within the required range.

The main electrical panel has AC protections for the grid-tied inverter and the vehicle charger (Figure 7). On the left side, a 20 Amp two-phase protection is shown for the L1 and L2 signals of the on-grid inverter. At the bottom, a single-phase 120 Vac line protection is shown for powering the weather station. On the right side, a three-phase protection is shown for the L1, L2, and L3 signals of the vehicle charger.

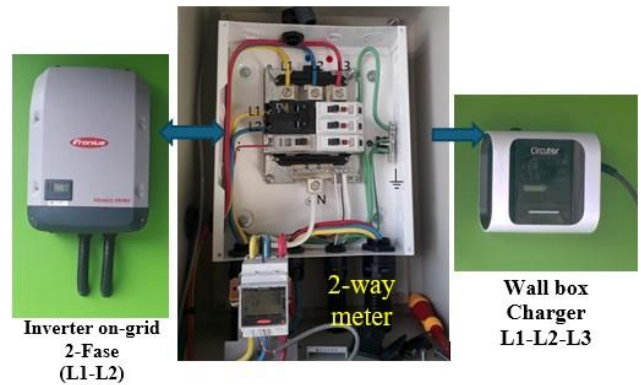


Fig. 7. Protection panel for the on-grid inverter and vehicle charger. Bidirectional smart meter for three-phase grid/load signal.

The vehicle charger will demand power in one direction. The inverter operates in both directions; on one hand, it converts the DC electricity from the PV system to the AC distribution system, when there is radiation, and on the other hand, it will demand the required energy to keep functioning. The smart meter is bidirectional, so it records the power delivered to, or demanded from, the distribution system. A positive energy balance (excess delivered to the distribution system) will translate into energy savings and positive environmental impact, a fundamental objective of the system.

For loads other than the three-phase vehicle charger, a power outlet was installed to allow connection of equipment for Modes 1 and 2 charging technology. A 120 V AC outlet will also allow charging of portable devices and cell phones, in addition to the multiplexer required to tap into the available network point. The network signals are necessary for remote data monitoring of the inverter, vehicle charger, and weather station. Therefore, a switching circuit was devised to enable, with a single outlet, the availability of single-phase (120 V AC) and

two-phase (208 VAC) signals. The circuit shown in Figure 8 was designed and implemented.

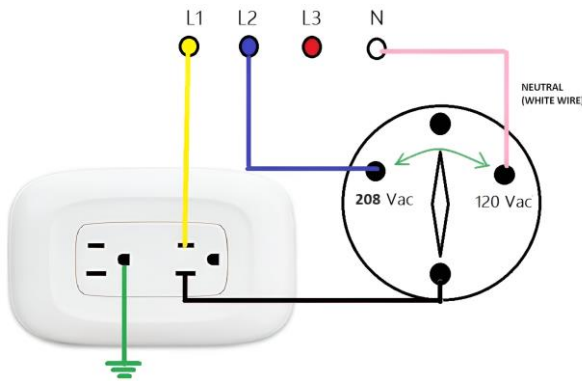


Fig. 8. Voltage selector connection circuit 120 / 208 V AC.

As can be seen, it can be switched to obtain Line to Line voltages (208 V AC) and Line to Neutral voltages (120 V AC). The center terminal is connected to ground, as required by the standard. Although it is a circuit that simplifies and enables the provision of both voltages, it should be regularly kept at 120 V AC to avoid damage from unintended connection of equipment operating at 120 V AC and being connected to 208 V AC. Figure 9 shows an image of the assembly performed.

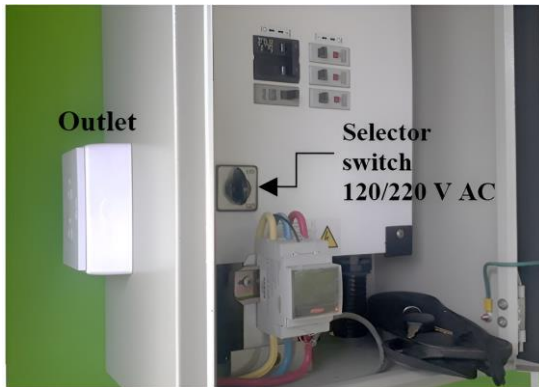


Fig. 9. Assembly of 120/208 V AC voltage selector and power outlet.

4. Performance Evaluation

The performance analysis of the electric charging station involves conducting vehicle charging sessions and measuring relevant variables. These measurements include the generated PV power, power demanded by the vehicle, solar radiation, and power delivered to the distribution system. To conduct these measurements, a Renault Kangoo ZE electric vehicle with the following specifications was utilized:

Table I. Renault Kangoo ZE specifications

Electric motor technology	Permanent magnet
Maximum power CV	60 CV (59,2 HP)
Top speed	135 km/h
Standardized consumption	15,5 Wh/km
On-board energy	33 kWh
New European Driving Cycle driving range	270 km

Figure 10 displays the curves of relevant variables observed during tests aimed at calculating the energy balance over a typical solar cycle. It's noteworthy that the test day experienced partial sunshine in the morning followed by rain in the afternoon.

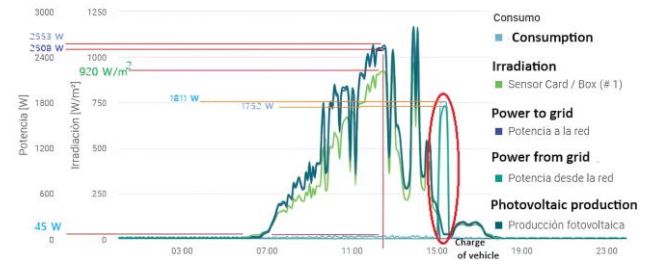


Fig. 10. Curves of relevant variables observed during the charging process of the electric vehicle.

The irradiation, and consequently the generation, can be observed throughout the solar cycle from 6:00 am to 6:00 pm, with peaks occurring at 12:30 pm and reaching a maximum value at 2:05 pm (980 W/m²). The initial analysis conducted focuses on the efficiency of the PV system. For this purpose, a reference time instant (12:30 pm) has been selected. At this moment, the following data is recorded: PV production 2553 W, power delivered to the distribution system 2508 W, irradiation 920 W/m², consumption 45 W, and power drawn from the distribution system 0 W. Notably, there is no demand from the distribution system due to the low consumption compared to the PV generation. It's important to note that the PV generation equals the power supplied to the distribution system plus the demanded power (2508 W + 45 W = 2553 W).

The panel array consists of 9 panels, each measuring 2 m x 1 m. This represents a capture area of 18 m². Therefore, at the time of analysis, the photovoltaic capture power, according to the recorded radiation, should be: 920 W/m² x 18 m² = 16560 W. The efficiency can then be estimated as 2553 W/16560 W x 100 % = 15,4 %.

The manufacturer records an efficiency of 19% under ideal conditions, with radiation of 1000 W/m² and a panel temperature of 25°C (at the time of measurement, the module temperature was 47°C). However, despite the environmental conditions being different from ideal, the difference in efficiency is due to the suboptimal positioning of the panel array concerning the incidence of solar radiation throughout the day. It should be mentioned that the radiation sensor captures radiation in a focused manner (the movement of the sun does not affect it), while the photovoltaic array is not optimally directed towards the south. Instead, due to the roof's location, its orientation was restricted to southwest, with the appropriate inclination according to the latitude. The roof orientation mostly limits the orientation of the panel array on it. The reasons are more related to aesthetics, which requires synchronizing roof-panel orientation, and the difficulty of assembling supports on the roof for panels with different orientations.

It is important to mention that the variation of the panel temperature with respect to the standard measurement temperature (25°C) can be a factor to consider in efficiency reduction. Figure 11 presents the curves of ambient temperature, panel temperature, and radiation for the day of analysis.

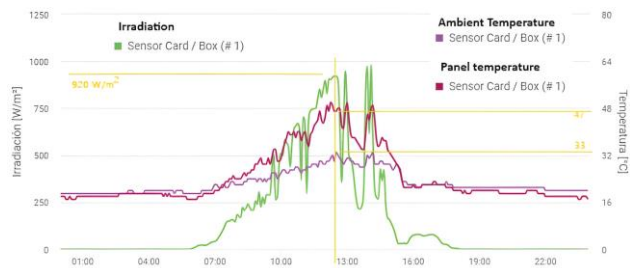


Fig. 11. Effect of ambient temperature and radiation on panel temperature.

It's notable that radiation influences the ambient temperature, and the latter increases the panel temperature. At the reference time (12:30 h), the radiation of 920 W/m² and ambient temperature of 33°C cause a panel temperature of 47°C. It should be mentioned that on this day, the wind speed was practically zero, preventing the possibility of cooling. On the other hand, when radiation decreases due to cloud cover, the module temperature decreases much more abruptly than the ambient temperature. When radiation decreases completely (before 6 am or after 6 pm), the module temperature remains slightly below the ambient temperature. However, for these temperature ranges, this variable does not appear to be as influential on photovoltaic generation, which is predominantly influenced by irradiation. The range of ambient temperature fluctuated, for the analysis day, between 19°C and 33°C, and the panel temperature between 17°C and 50°C. These variations do not significantly affect the system's efficiency.

Now, concerning the vehicle charging time (Figure 11), the energy balance can be estimated. The vehicle charging started at 15h and ended at 15h35'. At the time of charging, there was heavy cloud cover reducing radiation values. Therefore, the demand from the distribution system was considerable. At 15h20', the power demanded by the vehicle, through the vehicle charger, was 1811 W. The availability of radiation was only 30 W/m², resulting in a PV generation of 59 W. Therefore, the power from the distribution system was 1.752 W. In this case, the demanded power is the PV generation plus the power coming from the distribution system (59 W + 1.752 W = 1.811 W).

The energy is obtained by integrating (area under the curve) of the power graphs in Figure 11. This utilizes the daily records provided by the implemented monitoring platform. Figure 12 shows the energy results of consumption and total generated energy. It is notable that the generated value is much higher than the consumed value, with a positive balance of 10,12 kWh (11,34 kWh – 1,22 kWh = 10,12 kWh). On the remaining days (where there was no vehicle charging), the station's consumption

has been close to 0.32 kWh (consumption of LED lighting). Therefore, the energy consumed by the vehicle can be estimated at 1.22 kWh - 0.32 kWh = 0.9 kWh. This charge represents 21% of the battery's full capacity. The charging time performed was 35 minutes, resulting in an estimated remaining time for full charge of 166 minutes (2 hours 46 minutes). According to the graph shown, the full charge of the Kangoo ZE vehicle (33 kWh) could be achieved with a net zero balance, with 3 days of average radiation. Naturally, this vehicle does not cover the 240 km daily, resulting in a positive balance at the end of the month, depending on the number of charges and the frequency of their occurrence.



Fig. 12. Total PV generation and energy demanded by EV.

5. Economic analysis

The Table II presents the associated costs.

Table II. Costs involved in the system.

Initial Investment			
	Unit cost USD	Quantity	Cost USD
Photovoltaic panels	100	9	900
Inverter on-grid	900	1	900
Wiring and electrical components	250	1	250
Structure and assembly	200	1	200
Total (USD)			2.250

The investment return is calculated in the following way:

Delivered power of system: 3,6 kW
 Cost per installed Watt: 0,625 USD / Watt
 Delivered energy/month: 3,6 kW x 4 HPS x 30 = 432 kWh
 Energy monthly cost (approximate): 0,1 USD / kWh
 Energy monthly equivalent value: 0,1 USD x 432 = 43,2 USD
 Time to recover the investment:
 2.250 USD / \$ 43,2 USD = 52,1 months (4,3 years)

Table III presents the savings represented by owning an electric vehicle instead of an internal combustion vehicle. For this purpose, the reference autonomy values of the electric vehicle have been considered.

Table III. Comparison of fuel vehicle vs. electric vehicle

Range	200	km
Standardized consumption (battery)	12	kWh
Energy cost (0,1 USD / kWh)	1,2	USD
Consumed fuel	5	Gallons
Fuel cost (3,9 USD / gallon)	19,5	USD
Saving by kWh (19,5 – 1,2) USD / 12	1,525	USD

If all the energy produced by the PV system were used for vehicle charging, the total savings over a month would be: $1,525 / \text{kWh} \times 432 \text{ kWh/month} = 656 \text{ USD} / \text{month}$

In this case, the accumulated monthly savings from PV system and electric mobility would be: $656 \text{ USD} + 43,2 \text{ USD} = 700 \text{ USD}$

An interesting index is the ratio of electrical (kWh) and fuel consumption (Liter). In this case, it is: $12 \text{ kWh} / (3,78 \times 5) = 0,635 \text{ kWh} / \text{Liter}$.

Studies conducted by the Ministerio de Minas y Energía in Colombia and the Unidad de Planeamiento Minero Energético (UPME) [6], [7] have established that electricity generation produces a carbon footprint of 164,38 gCO₂ per kWh. However, studies such as the one presented in [7] have shown that a PV system generates 29,8 gCO₂ per kWh. Thus, an estimated carbon footprint savings of 134,6 gCO₂/kWh could be calculated, considering the monthly energy production of the system: $134,6 \times 432 \text{ kWh/month} = 58.147 \text{ gCO}_2 / \text{month}$ avoided.

6. Conclusions

This paper emphasizes the importance of photovoltaic EV charging stations in reducing carbon emissions and promoting sustainable mobility. By combining the advantages of EV technology with renewable energy sources, we can pave the way towards a cleaner, more sustainable future for transportation, thereby contributing to global efforts to combat climate change and preserve the health of our planet.

The paper discusses key factors to consider when designing photovoltaic EV charging stations, such as location selection, solar panel orientation, charging infrastructure requirements, grid integration, and scalability.

Furthermore, the architecture of the system and how its components (including solar panels, inverters, batteries, charging stations, and control systems) interact with each other are detailed and explained.

Finally, the paper presents the results of performance evaluations, including efficiency, charging capacity, and environmental impact. Additionally, a comparison of the performance of solar-powered EV charging stations with conventional grid-powered stations is provided.

References

- [1] G. C. Mouli, P. Bauer, and M. Zeman, "System design for a solar powered electric vehicle charging station for workplaces," *Applied Energy*, vol. 168, pp. 434-443, 2016.
- [2] K. Satya Prakash Oruganti, C. Aravind Vaithilingam, and G. Rajendran, "Design and sizing of mobile solar photovoltaic power plant to support rapid charging for electric vehicles," *Energies*, vol. 12, no. 18, p. 3579, 2019.
- [3] K. Habib, M. Hasan, S. Karmakar, and M. Rabbani, "Performance analysis of solar charging station for electric vehicle: A case study based on 21.1 kwp solar charging station in Bangladesh," *International Journal of Scientific and Engineering Research*, vol. 11, no. 2, pp. 195-198, 2020.
- [4] I. E. Atawi, E. Hendawi, and S. A. Zaid, "Analysis and design of a standalone electric vehicle charging station supplied by photovoltaic energy," *Processes*, vol. 9, no. 7, p. 1246, 2021.
- [5] S. D. Prasetyo, F. J. Regannanta, M. S. Mauludin, and Z. Arifin, "Economic feasibility of solar-powered electric vehicle charging stations: A case study in Ngawi, Indonesia," *Mechatronics and Intelligent Transportation Systems*, vol. 2, no. 4, pp. 201-210, 2023.
- [6] X. González, "En Colombia el Factor de Emisión de CO₂ por Generación Eléctrica es de 164, 38 Gramos por kWh," *Diario La República*, [Online]. Available: <https://www.larepublica.co/especiales/colombia-potencia-energetica/en-colombia-el-factor-de-emision-de-co2-por-generacion-electrica-es-de-16438-gramos-por-kwh-2966236>
- [7] J. S. Rippe, O. G. Mora, P. Dávila, J. G. Ortiz, H. H. Flórez, and I. G. Reyes, "Cálculo del factor de emisiones de la red de energía eléctrica en Colombia," [Online]. Available: https://www1.upme.gov.co/ServicioCiudadano/Documents/Proyectos_normativos/Documento_Tecnico_FE_2020.p df
- [8] I. Arnabat, "Cuál es la huella de carbono de un captador solar térmico y de un panel fotovoltaico," *caloryfrio.com*. <https://www.caloryfrio.com/energias-renovables/energia-solar/cual-huella-dcarbono-de-un-captador-solar-termico-y-de-un-panel-fotovoltaico.html> (accessed Aug. 12, 2024).